

# Study of preparation parameters of powder and pelletized Pt/KL catalysts for *n*-hexane aromatization

Gary Jacobs, Walter E. Alvarez, Daniel E. Resasco\*

*School of Chemical Engineering, University of Oklahoma, Norman, OK 73019, USA*

Received 22 December 1999; received in revised form 4 May 2000; accepted 5 May 2000

## Abstract

Pt/KL powder and pelletized catalysts were synthesized by different methods including ion exchange (IE), incipient wetness impregnation (IWI), and vapor phase impregnation (VPI) methods. A detailed characterization was conducted on the various samples in order to determine the distributions of Pt particle size and location resulting from each preparation, as well as the relationships between these distributions and the catalytic performance. The catalysts were pretreated at two different reduction temperatures — 400 and 500°C — to investigate the sensitivity of each catalyst to thermal treatment. All catalysts showed high dispersion, with H/Pt ratios greater than unity. However, FTIR of adsorbed CO showed that more important than dispersion, it is the distribution of Pt cluster size and location, which influences the resulting catalytic stability. Standard IE catalysts were found to have a high fraction of Pt particles external to the L-zeolite and were the most sensitive to thermal treatment, displaying Pt migration out of the L-zeolite. These catalysts deactivated rapidly by coke formation. The addition of excess K<sup>+</sup> ions in the exchange solution and a longer aging period, as suggested in the patent literature, improves the Pt dispersion.

IWI and VPI catalysts showed a majority of Pt clusters inside the L-zeolite channels. However, after high temperature reduction treatment, the IWI catalysts displayed particle growth inside the channels, in contrast with the VPI. The IWI catalysts were found to deactivate to about half their initial activity, while the VPI maintained the highest activity and stability. Different VPI methods including a moderate vacuum and a helium flow technique were examined and they showed similar Pt cluster distributions and catalytic performance to the catalysts synthesized using high vacuum. Preparation directly on the pellet for the methods investigated in this work (standard IE, IWI, and VPI) resulted in large fractions of Pt clusters external to the pores and likely on the binder. Thus, rapid deactivation by coke formation was evident. These results indicate that pelletized catalysts prepared by any of these techniques would require preparation on the powder prior to pellet extrusion. © 2001 Elsevier Science B.V. All rights reserved.

*Keywords:* Pt/KL; Aromatization; *n*-Hexane; DRIFTS; Vapor phase impregnation

## 1. Introduction

Over the past 20 years, researchers have used different methods to prepare Pt/KL catalysts for the aromatization of *n*-hexane reaction. These typically

involve ion exchange (IE), incipient wetness impregnation (IWI) and more recently, vapor phase impregnation (VPI) methods [1–8]. These procedures result in catalysts with differences in the distributions of Pt particle size and location. The first consideration is the residual acidity that may remain on the zeolite after each preparation. Therefore, for the IE catalysts, a back-exchange procedure is necessary in order to exchange out Bronsted sites arising from reduction

\* Corresponding author. Tel.: +1-405-325-4370;

fax: +1-405-325-5813.

*E-mail address:* resasco@ou.edu (D.E. Resasco).

of  $\text{Pt}^{2+}$  exchanged in the zeolite, as described by Ostgard et al. [2]. In contrast, less residual acidity is generated for IWI catalysts during the reduction step, because there is little exchange with the L-zeolite during preparation. Coimpregnation of KCl during the IWI step to reduce Bronsted acidity displayed an increased selectivity to benzene. Finally, the VPI method avoids the exchange of  $\text{K}^+$  with Bronsted sites altogether [6].

The second important aspect to consider is the size and location of the Pt clusters in the zeolite. The preparation method is critical to the distribution of the Pt clusters and directly influences the stability of the catalyst under aromatization conditions. Previous studies have demonstrated the sensitivity of the calcination temperature during preparation [9,10]. Calcination at temperatures higher than  $400^\circ\text{C}$  resulted in a large fraction of external Pt. Pt particles located external to the L-zeolite channels are susceptible to bimolecular reaction pathways that lead to formation of coke, but those inside the channels are protected from these reactions [11]. The morphology of the Pt clusters inside the channels also has a strong influence on the deactivation rate. Large clusters located inside the L-zeolite channels are more sensitive to agglomeration, resulting in blockage of the channels and entombment of Pt particles. On the other hand, small clusters located in the lobes of the channels are less sensitive to Pt growth. Results of methylcyclopentane ring opening (MCP-RO) for small Pt clusters indicated that the standard IE procedure results in a considerable fraction of Pt external to the channels of the L-zeolite [2]. The ring opening pattern of the MCP molecule is a good indicator of the morphology of the Pt/KL catalysts and of the location of the Pt clusters [10,12]. For small Pt clusters supported on a nonmicroporous material, the MCP molecule will form 2MP, 3MP, and *n*-hexane in the statistical ratio 40%:20%:40%. However, for Pt clusters small enough to reside inside the microporous channels but large enough to partially block them, as is the case for the Pt/KL catalyst prepared by IWI, the MCP molecule is collimated by the channels such that there is preferential cracking to form 3MP. Therefore, the 3MP/2MP ratio is higher than the statistical distribution. If the Pt clusters remain outside the channels, on the external surface of the L-zeolite, the ratio is closer to statistical. Similarly, a TPR investigation of catalysts

calcined at  $400^\circ\text{C}$  [2] demonstrated that IE catalysts displayed a greater fraction of platinum in the form of  $\text{Pt}^{2+}$  ions coordinated to the zeolite walls, while IWI catalysts predominantly showed  $\text{Pt}^{4+}$  species in the form of  $\text{PtO}_2$  clusters located inside the channels. From MCP-RO testing, less Pt was found on the exterior surface of the L-zeolite for the IWI catalysts than in the case of the IE [2]. However, although most of the Pt resides inside the L-channels after IWI preparation, a fraction of particles inside the pores were found to be large enough to cause pore blockage, as evidenced by TEM and pulse MCP ring opening [12]. In that case, the 3MP/2MP ratio was considerably higher than the statistical distribution, indicating that the MCP molecule showed preferential bond cleavage due to collimation of the molecule by the zeolite channels and cracking on internal, but relatively large, Pt clusters.

The liquid to solid ratio in the impregnation procedure is an important parameter that many times is not properly considered. In this work, we examine the sensitivity of this parameter more closely by preparing IWI catalysts with different levels of hydration of the L-zeolite both prior and during incorporation of the loading solution.

In our previous studies, catalysts prepared by the VPI procedure were found to be more active and selective with much greater stability than the IWI and IE catalysts. Results of EXAFS for series of equal loadings of Pt prepared by IWI and VPI showed that the Pt clusters resulting from the VPI preparation had lower Pt–Pt coordination and higher coordination to the zeolite lattice oxygen [12]. At the same time, these catalysts showed about half the amount of coke as the IWI catalysts [13], as well as a lower deactivation under aromatization reaction [12].

In this contribution, we have conducted a systematic comparison of the different preparation methods, analyzing the distribution of Pt clusters resulting from each method, and its direct influence on the stability of Pt/KL catalysts. Three methods were compared — standard IE, IWP, and VPI. FTIR of adsorbed CO and hydrogen chemisorption were employed as characterization techniques. Results from this characterization were correlated with the deactivation patterns of the catalysts under the *n*-hexane flow reaction. As we have demonstrated before, the catalysts prepared by the VPI method show the highest

activity, selectivity, and stability for *n*-hexane aromatization [12]. However, the VPI method previously studied involves the use of high vacuum, which is not very convenient for commercial applications. Therefore, we investigated slight modifications to the method to make it more suitable for industrial practice.

## 2. Experimental

### 2.1. Catalyst preparation

The K-LTL zeolite powder (series TSZ-500, BET area 292 m<sup>2</sup>/g, SiO<sub>2</sub>/Al<sub>2</sub>O<sub>3</sub> ratio=6) was provided by Tosoh Company. Pellets were extruded using 10% K-Sil binder and 1.5% stearic acid. Prior to incorporation of Pt metal, the zeolite powder or pre-formed pellet was dried in an oven at 110°C for 12 h and calcined at 400°C for 5 h. All calcination steps were performed under flow of air (100 cm<sup>3</sup>/g zeolite), employing a temperature ramp of 3°C/min. Incorporation of platinum metal into the zeolite was performed using the following three methods:

#### 2.1.1. Standard ion exchange (SIE) method

In the ion exchange method, tetraammine platinum(II) nitrate salt (Alfa Aesar) was used as the precursor. For the 0.5% Pt/KL catalyst, the precursor was added dropwise over an 8 h period to the 200 ml agitated suspension of L-zeolite. The slurry was further stirred for 24 h, filtered using a Buchner funnel, and dried at room temperature. The catalyst powder was further dried in an oven at 110°C for 12 h and calcined at 350°C for 2 h under flow of air. The calcined sample was reduced at 400 or 500°C under flow of hydrogen. This catalyst was designated as SIE-PWD-NBE for 'not back-exchanged'. In order to remove residual acidity generated during the reduction step, a portion of the catalyst was back-exchanged using an aqueous solution of 0.01 M KNO<sub>3</sub> added dropwise over 8 h. The catalyst was then filtered again, dried, and re-calcined. This catalyst was designated as SIE-PWD-BE for 'back-exchanged'. In the case of the preparation on the KL pellets, the same procedure was used, except that the pellets were suspended in a Teflon basket to prevent attrition. This catalyst was designated SIE-PEL-NBE.

#### 2.1.2. Modified Ion exchange (MIE) method

An Exxon process patent [14] claims that contacting the L-zeolite with an aqueous loading solution containing soluble Pt salt as well as additional K<sup>+</sup> cations assures that acid sites are not formed on the catalyst during the drying step. More specifically, the amount of K<sup>+</sup> cation initially present in combination with the platinum salt in the loading solution is such that after loading, the initial amount of the K<sup>+</sup> plus the amount of K<sup>+</sup> cation added to the solution by ion exchange of the platinum salt with the L-zeolite is present in the loading solution in a concentration equal to the concentration of K<sup>+</sup> metal salt added to the solution by ion exchange between the platinum salt and the L-zeolite at incipient wetness. Our preparation following the guidelines of Poeppelmeier et al. [14] is provided below for clarity. We employed tetraammine platinum(II) chloride as the source salt, and additional K<sup>+</sup> was added to the loading solution from KCl source. Furthermore, a critical aging step is also described whereby excess liquid is removed from the carrier and the solids are allowed to be aged for a time at the prescribed temperature. The patent claims that this aging step allows the platinum to migrate and uniformly distribute throughout the L-zeolite. Afterwards, the catalyst is dried and calcined, prior to the reduction step. For 10 g of KL, 0.17 g of Pt(NH<sub>3</sub>)<sub>4</sub>Cl<sub>2</sub> was required. Since each mole of Pt<sup>2+</sup> cation displaces 2 mol of K<sup>+</sup> from the L-zeolite support during ion exchange, an additional 1.03 × 10<sup>-3</sup> mol of K<sup>+</sup> was included in the loading solution. The volume of solution required to reach incipient wetness for 10 g of KL was 6.9 ml. The total volume of loading solution was 17 ml, so the required amount of K<sup>+</sup> to be added to the initial loading solution was calculated to be 1.5 × 10<sup>-3</sup> mol. This corresponded to 0.112 g of KCl. After circulating the solids for 75 min, the wet solids were collected and aged at 50°C for 72 h in a closed vessel. The solids were then dried and calcined at 110°C for 16 h, further calcined at 200°C for 2 h, and again calcined further at 350°C for 3 h according to the recipe. This catalyst was designated MIE-PWD.

#### 2.1.3. Incipient wetness impregnation (IWI) method

In the IWI procedure, the freshly calcined support was quickly transferred to an inert atmosphere and impregnated dropwise while grinding with an aqueous solution of platinum salt tetraammine platinum(II)

nitrate. To achieve incipient wetness, a liquid/solid ratio of  $0.69 \text{ cm}^3/\text{g}$  was used. After impregnation, the samples were dried for 12 h at  $110^\circ\text{C}$  and then calcined for 2 h in air at  $350^\circ\text{C}$ . This sample was designated IWI-PWD. To analyze the effect of introducing excess water during the procedure, three additional catalysts were synthesized. In the first case (IWI-PWD-EXP), after calcination, the L-zeolite was exposed to ambient conditions for 12 h, so water from the ambient humidity penetrated in the pores. In this case, the pores were still filled to incipient wetness by using only the required liquid to solid ratio measured separately, which in this case was lower (i.e.  $0.49 \text{ cm}^3/\text{g}$ ). In the second case (IWI-PWD-XS), after calcination, the L-zeolite was again exposed to ambient conditions for 12 h, but now the original  $0.69 \text{ cm}^3/\text{g}$  ratio was used. Therefore, the pores were overfilled beyond incipient wetness. Finally, in the third case (IWI-PWD-NCL), the L-zeolite was dried at  $110^\circ\text{C}$ , but not calcined. The same  $0.69 \text{ cm}^3/\text{g}$  was employed during impregnation, resulting in overfilling of the pores. In each modification, the resulting catalysts were dried and calcined in the usual way.

For the case of impregnation on the KL pellets, the extrudates were dip impregnated by lowering the perforated Teflon basket containing dehydrated L-zeolite into solution and removing quickly. This sample was named IMP-PEL. The resulting Pt loading was in this case only 0.57 wt.%.

#### 2.1.4. Vapor phase impregnation (VPI) method

The third method employed was VPI [4,5]. After quickly transferring the freshly calcined support to an inert atmosphere, platinum acetylacetonate (Alfa Aesar) was physically well-mixed with the KL, and then the solid mixture was transferred to a reactor tube (sealed at one end). The reactor tube was sealed under vacuum and evacuated for 12 h to below  $10^{-5}$  Torr, using a turbomolecular pump. The catalyst was slowly ramped to  $80^\circ\text{C}$  and held at this temperature for 1 h as a precaution to remove traces of impurities. For example, impurities might include weakly physisorbed water resulting from exposure to ambient conditions during transfer operations, which could be removed below the temperature of sublimation. The catalyst was then ramped to  $100^\circ\text{C}$  and held for 1 h to sublime the  $\text{Pt}(\text{AcAc})_2$ , at which point the pressure increased significantly. After sublimation, the catalyst

was ramped to  $130^\circ\text{C}$  and held for 15 min to ensure that virtually all of the  $\text{Pt}(\text{AcAc})_2$  was sublimed. The reactor tube was cooled to room temperature, and the sample was removed. At this point, the sample was light yellow in color, indicating that the  $\text{Pt}(\text{AcAc})_2$  did not decompose during the procedure. To decompose the platinum precursor, the sample was ramped to  $350^\circ\text{C}$  in flow of air and calcined for 2 h. This sample was designated VPI-PWD-HV for high vacuum preparation. It is important to note that it is important during the preparation to dehydrate the L-zeolite and keep it very dry during the entire procedure. At no point during the preparation or storage of the catalyst should the L-zeolite or the Pt acetylacetonate be allowed to contact with moisture.

To examine more convenient methods for preparing VPI catalysts in a large scale, we examined two additional preparation methods. The first one (VPI-PWD-MP) was prepared using a mechanical pump to achieve a moderate vacuum (about  $10^{-3}$  Torr). The second one (VPI-PWD-HEF) was done performing the sublimation at atmospheric pressure under a low flow rate of He ( $<10 \text{ cm}^3/\text{min}$ ). For the case of the pellets (VPI-PEL-HEF), the low helium flow method was used. The Pt loadings were determined by ICP analysis after complete dissolution of the samples in aqua regia/HF solution at Galbraith Laboratories. A summary of the catalysts, nomenclature, and measured loading, is presented in Table 1.

#### 2.2. Catalyst characterization

Hydrogen chemisorption measurements were conducted on several of the powder preparation catalysts in a static volumetric adsorption Pyrex system, equipped with a high capacity, high vacuum pumping station that provided vacuum on the order of  $10^{-9}$  Torr. The amount of reversibly adsorbed hydrogen was quantified in the following manner. After obtaining the first isotherm, the sample was evacuated for 5 min at room temperature and a second isotherm was determined. The irreversible H/Pt was obtained by subtracting the two isotherms.

Infrared spectroscopy of adsorbed CO was performed on a Bio-Rad FTS-40 spectrometer, equipped with a MCT detector. Experiments were conducted in a diffuse reflectance cell from Harrick Scientific, type HVC-DR2 with ZnSe windows that allowed us

Table 1  
Summary of catalysts and loadings

Catalyst description	Catalyst designation	Pt loading (%)
Standard ion exchange with no back-exchange	SIE-PWD-NBE	0.50
Standard ion exchange with back-exchange of potassium	SIE-PWD-BE	0.50
Modified ion exchange	MIE-PWD	0.50
Incipient wetness impregnation	IWI-PWD	1
Incipient wetness impregnation with prior exposure of L-zeolite to ambient conditions	IWI-PWD-EXP	1
Incipient wetness impregnation with prior exposure of L-zeolite to ambient and overfilling	IWI-PWD-XS	1
Incipient wetness impregnation without calcination of L-zeolite resulting in overfilling	IWI-PWD-NCL	1
Vapor phase impregnation using high vacuum	VPI-PWD-HV	1
Vapor phase impregnation using moderate vacuum (mechanical pump)	VPI-PWD-MP	1
Vapor phase impregnation using low helium flow	VPI-PWD-HEF	0.89
Standard ion exchange of L-pellets using basket	SIE-PEL-NBE	0.51
Dip impregnation of L-pellets using basket	IMP-PEL	0.57
Vapor phase impregnation of L-pellets using low helium flow	VPI-PEL-HEF	0.65

to perform in situ thermal pretreatments. For each IR spectrum, taken at a resolution of  $8\text{ cm}^{-1}$ , 128 scans were added. Samples were pre-reduced ex situ under  $\text{H}_2$  flow at either 400 or 500°C for 1 h. Prior to each spectrum, the catalyst was re-reduced in situ in a flow of  $\text{H}_2$  for 30 min at 300°C, cooled under He flow, and purged in He at room temperature for 30 min. The background was recorded at this time. Then, the catalyst was exposed to a flow of 3% CO in He for 30 min at room temperature and purged in He for 30 min, prior to obtaining the scans, to remove the contributions from gas phase and weakly adsorbed CO.

### 2.3. Catalytic activity

Steady-state *n*-hexane reaction testing was conducted in a continuous-flow reactor. The reactor consisted of a 0.5 in. stainless steel tube with an internal thermocouple. The experiments were conducted using 0.40 g of catalyst in each run. Although preparation of the pelletized samples was conducted on the extrudates, the pellet was crushed into powder for the catalytic activity tests. Each catalyst was sieved to give particle sizes between 300 and 425  $\mu$  (40/50 mesh granules). The catalyst bed was supported on a bed of quartz glass wool. The reactor was operated under flowing hydrogen. *n*-Hexane (Aldrich, <99% purity) was added by infusion with a syringe pump (Sage model M365) through a tee-junction prior to the reactor. In all experiments, the hydrogen/*n*-hexane ratio was kept at 6.0. Prior to reaction, the catalyst

was slowly ramped in flowing hydrogen at  $100\text{ cm}^3/\text{g}$  catalyst for 2 h to a temperature of 450°C (except where otherwise noted). Reaction testing was conducted at a WHSV of  $10\text{ h}^{-1}$  at atmospheric pressure and a temperature of 450°C, unless otherwise noted.

A purge-valve was used to automatically send samples to a gas chromatograph for analysis. The gas chromatograph utilized helium as the carrier gas and sent purged products of reaction through the HP-PLOT/ $\text{Al}_2\text{O}_3$  'S' deactivated capillary column to achieve product separation. Products were detected using a flame ionization detector (FID). A nonlinear 1.5 h temperature ramp from 40 to 200°C provided the means for adequate peak separation in the GC column.

## 3. Results

### 3.1. Catalyst characterization

#### 3.1.1. Hydrogen chemisorption

The H/Pt results obtained on the powder samples after reduction at either 400 or 500°C are reported in Table 2. As in previous reports [5,15], very high H/Pt values were obtained. A significant difference was obtained between the total and the irreversible adsorption values, showing that in all cases, contributions from weakly adsorbed hydrogen were significant. Nonetheless, high irreversible H/Pt values, above 1.0 were observed in all cases, indicating very high metal dispersion in all the samples, particularly in the VPI

Table 2  
Results of hydrogen chemisorption for powder catalysts

Catalyst	H/Pt total reduction at 400°C	H/Pt irreversible reduction at 400°C	H/Pt total reduction at 500°C	H/Pt irreversible reduction at 500°C	Difference between R500 and R400
SIE-PWD-NBE	1.8	1.3	1.5	1.0	0.3
IWI-PWD	1.9	1.6	1.5	1.2	0.3
IWI-PWD-EXP	1.8	–	1.5	–	0.3
IWI-PWD-XS	1.8	–	1.4	–	0.4
IWI-PWD-NCL	1.5	–	0.9	–	0.6
VPI-PWD-HV	2.0	1.7	1.7	1.4	0.3
VPI-PWD-MP	2.0	–	1.7	–	0.3
VPI-PWD-HEF	2.0	–	1.7	–	0.3

catalysts. By increasing the reduction temperature from 400 to 500°C, clear drops in H/Pt values were observed for all samples.

Interestingly, in general, for the IE, IWI, and VPI powder catalysts, the losses were approximately the same for each case. However, the IWI catalysts prepared with excess water (IWI-PWD-XS and IWI-PWD-NCL) displayed a higher sensitivity to reduction temperature. Finally, no differences were detected among the H/Pt values for all the different vapor phase preparation methods tested, indicating that the three VPI methods were similarly effective in dispersing Pt.

### 3.1.2. Infrared spectroscopy

It has been shown that FTIR of adsorbed CO is an important tool to probe the state of Pt clusters in Pt/KL [12,16]. In comparison with Pt/SiO<sub>2</sub> catalysts, which typically display a well-defined sharp peak at around 2074 cm<sup>-1</sup> for the stretching frequency of linearly adsorbed CO, Pt/KL catalysts display complex bands which typically extend from 2080 cm<sup>-1</sup> to much lower wavenumbers (e.g. as low as 1930 cm<sup>-1</sup>). In a previous paper [12], we utilized DRIFTS of adsorbed CO to compare the morphology of Pt particles inside the KL zeolite, prepared by IWI and VPI methods. In that case, our results agreed very well with the hypothesis that CO itself modifies the structure of the small Pt clusters inside the KL zeolite. For a typical Pt/KL sample, we have observed that during the first few minutes, a band developed centered at about 2068 cm<sup>-1</sup>. However, only after 10 min did we see new bands emerging at about 2057 and 2014 cm<sup>-1</sup>. Even later, we observed the formation of additional bands at 1975 cm<sup>-1</sup> and lower. It was concluded that

CO adsorption does not probe the small metal particles in their original structure, but rather generates by disruption over time new molecular arrangements that are stabilized inside the zeolite.

In support of this idea, Stakheev et al. [16] have tabulated the reproducibility of the position of these bands from several authors, and suggested that several different molecular species were formed with distinct stoichiometric ratios of Pt<sub>x</sub> and CO<sub>y</sub>. They proposed that during CO adsorption, Pt carbonyls can be formed and stabilized by the zeolite, which could act as a ligand. EXAFS data have shown that the 5–6 atom metallic particles present in the KL zeolite before the admission of CO, were completely disrupted, and Pt–CO species were formed [17,18]. It was also shown that saturation of CO was reached at 1 mbar P<sub>CO</sub> after approximately 30 min [16]. However, after increasing P<sub>CO</sub> to 500 mbar, the intensity of the bands increased by a factor of 5, giving clear evidence of Pt-carbonyl formation. The important point to notice is that the formation of Pt carbonyls can only occur when the Pt clusters are very small. The metal–metal bond strength is much lower than that of the bulk metal only for particles with less than 15–20 atoms. Therefore, one may not expect the Pt particles outside the zeolite to be converted to Pt carbonyls. Even though disruption of the small Pt clusters occurs, FTIR of adsorbed CO is still a useful technique for making general conclusions about the location (i.e. inside the L-zeolite or external) and distribution of the Pt clusters prior to disruption. For our purposes, the results are strongly consistent with the idea that the distribution of low wavenumber bands reflects the distribution of the size of Pt clusters located inside the channels of the L-zeolite.

In contrast, the bands at and above  $2075\text{ cm}^{-1}$  indicate the Pt external to the pores. Bands present between  $2050$  and  $2075\text{ cm}^{-1}$  are likely caused by the Pt clusters in the near surface region of the L-channels. In support of this assignment, Stakheev et al. [16] showed loss of Pt carbonyl bands and an increase in bands at these wavenumbers after several adsorption and desorption cycles, in which the temperature was increased to  $400^\circ\text{C}$ . Furthermore, in our previous work, we observed an increase in these bands after agglomeration of the Pt clusters in an IWI catalyst after conducting oxidation–reduction cycles [12]. In

agreement with these observations, TEM results have indicated the high tendency of small clusters of Pt to disrupt and agglomerate if small amounts of CO are present in the hydrogen during the reduction step, resulting in activity loss [19].

We first probed our best Pt/KL SIE, IWI and VPI powder catalysts at two reduction temperatures,  $400$  and  $500^\circ\text{C}$ . The results are depicted in Fig. 1a and b. As discussed above [2,16], exposure of very small Pt clusters to CO causes disruption of the cluster and the formation of mobile species stabilized by the zeolite. This disruption results in the appearance of low

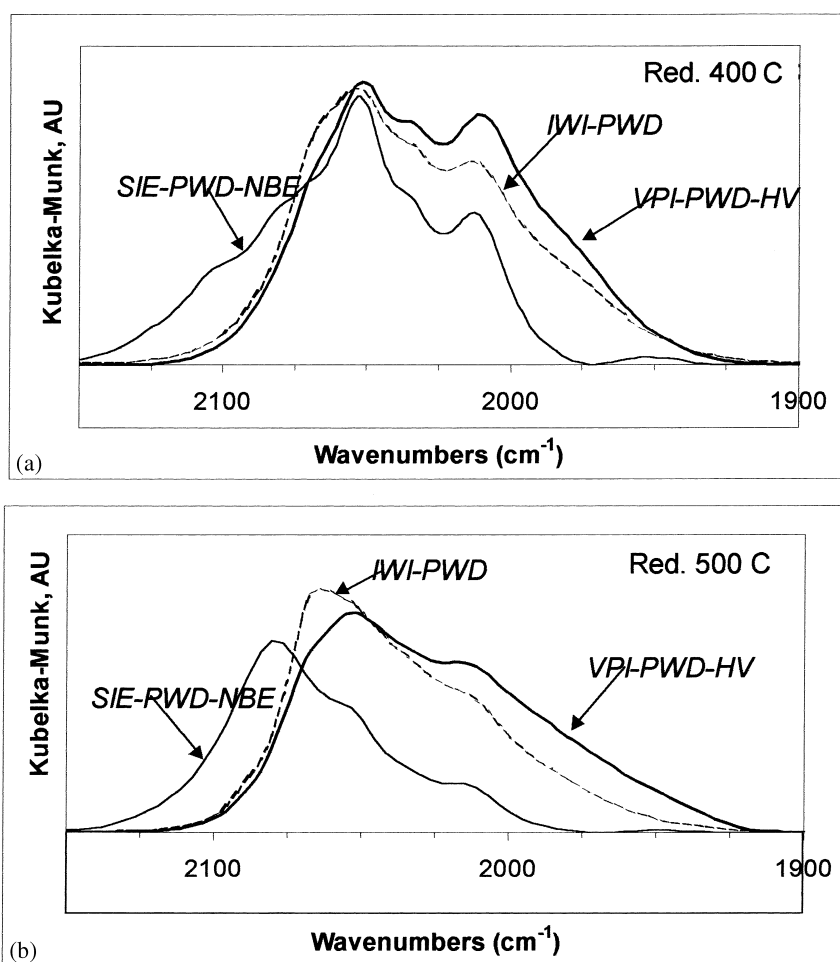


Fig. 1. (a) DRIFTS spectra of CO adsorbed on powder catalysts prepared by standard ion exchange without back-exchange (SIE-PWD-NBE), incipient wetness impregnation (IWI-PWD), and vapor phase impregnation high vacuum (VPI-PWD-HV) after reduction at  $400^\circ\text{C}$ . (b) DRIFTS spectra of CO adsorbed on powder catalysts prepared by standard ion exchange without back-exchange (SIE-PWD-NBE), incipient wetness impregnation (IWI-PWD), and vapor phase impregnation high vacuum (VPI-PWD-HV) after reduction at  $500^\circ\text{C}$ .

wavenumber bands for linear stretching. As reported in a previous study [12], we note again that the FTIR spectra changes as a function of CO exposure time, in agreement with the idea of Pt cluster disruption followed by stabilization inside the zeolite [16,20]. In order to make comparisons about the morphology of the Pt in the KL catalysts, for every sample we stopped CO exposure after exactly 30 min, and flushed in helium to remove gas phase CO.

For IWI-PWD and VPI-PWD-HV catalysts, Fig. 1a and b show that the positions of the bands resulting from the adsorption of CO were similar, extending from 2065 to 1930  $\text{cm}^{-1}$ . These bands are associated with Pt inside the channels of the L-zeolite [16]. As demonstrated by the low wavenumber bands (2010–1930  $\text{cm}^{-1}$ ) in Fig. 1a and b, the VPI catalyst displays higher capability than IWI and SIE catalysts for disrupting Pt clusters after reduction at both 400 and 500°C. No large differences were observed for IWI and VPI catalysts after reduction at 400°C. However, after reduction at 500°C, the IWI catalyst showed a larger decrease in bands associated with Pt-carbonyls and a more pronounced shoulder at 2065  $\text{cm}^{-1}$ , resulting in a shift to higher wavenumbers. In contrast with the IWI and VPI catalysts, the SIE-PWD-NBE catalyst did not show the bands related to the presence of small clusters/carbonyls. Also, this IE catalyst displayed bands which extended to frequencies higher than 2075  $\text{cm}^{-1}$ , indicating the presence of external Pt particles. The effect of reducing the catalyst at higher temperatures is severe. We observe a large decrease in intensity of the 2010, 2034, and 2053  $\text{cm}^{-1}$  bands, with a strong growth in intensity of the 2080  $\text{cm}^{-1}$  and higher frequency bands.

Although the bands for the Pt/KL catalysts are complex, the results of Fig. 1a and b were fitted by nonlinear least squares curve fitting using multiple Gaussians and are presented in Table 3 as a means of quantitative comparison. The spectra were divided into three regions to denote the three general morphologies. The band at 2080  $\text{cm}^{-1}$  corresponding to larger external clusters was fitted with a single Gaussian. The bands corresponding to clusters in the near surface region were fit with three Gaussians, with maxima centered at 2075, 2064, and 2053  $\text{cm}^{-1}$ , respectively. Finally, the Pt-carbonyl bands were fit with three Gaussians, with maxima centered at 2033, 2010, and 1975  $\text{cm}^{-1}$ .

We examined the effect of the back-exchange procedure on the standard ion exchange powder catalyst. As Fig. 2a indicates, no major differences in the band positions were noted for the back-exchanged catalyst SIE-PWD-BE, reduced at 400 and 500°C. After reduction at 400°C, in comparison with the SIE-PWD-NBE catalyst, however, there is a greater fraction of high wavenumber bands between 2075 and 2080  $\text{cm}^{-1}$  after back-exchange than before the procedure. In contrast, after reduction at 500°C, no large differences were observed before or after the back-exchange.

Fig. 2b shows a DRIFTS comparison of the standard IE with the modified IE catalyst prepared by the method of Poepelmeier et al. [14]. The modified IE catalyst displays a greater fraction of low wavenumber bands than the standard IE catalyst after reduction at 500°C, and shows virtually no bands associated with external Pt, in contrast with the standard IE catalyst. It is clear that the aging step during preparation aids in dispersing the salt throughout the channels. However, the VPI catalyst still presents a marked improvement

Table 3  
Percentage of total intensity for CO linear stretch vibration observed in DRIFTS spectra<sup>a</sup>

Catalyst	T (°C)	% Total intensity for CO linear stretch		
		2080 $\text{cm}^{-1}$	2050–2075 $\text{cm}^{-1}$	1930–2033 $\text{cm}^{-1}$
Standard ion exchange	400	25.1	45.3	29.6
Incipient wetness impregnation	400	0.0	49.4	50.6
Vapor phase impregnation (high vacuum)	400	0.0	45.9	54.1
Standard ion exchange	500	63.6	17.4	19.0
Incipient wetness impregnation	500	0.2	55.5	44.3
Vapor phase impregnation (high vacuum)	500	0.1	47.8	52.0

<sup>a</sup> Curve fitting was performed by fitting multiple Gaussians including one at 2080  $\text{cm}^{-1}$ , three in the range 2050 and 2075  $\text{cm}^{-1}$ , and three in the range 1930 and 2033  $\text{cm}^{-1}$ .

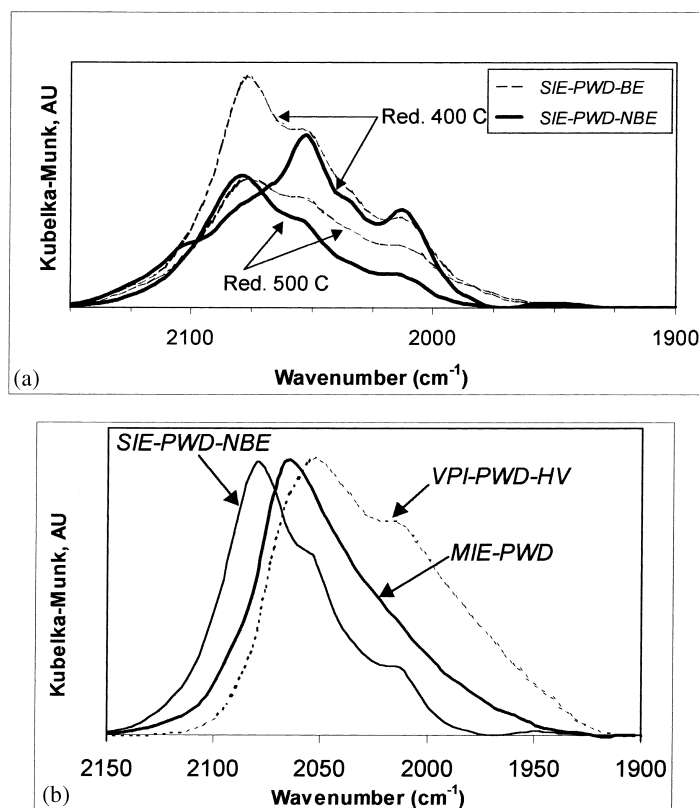


Fig. 2. (a) DRIFTS spectra of CO adsorbed on standard ion exchanged powder catalysts with and without back-exchange (SIE-PWD-BE and SIE-PWD-NBE, respectively) after reduction at 400 and 500°C. (b) DRIFTS spectra of CO adsorbed on ion exchanged catalysts prepared by the standard ion exchange method without back-exchange (SIE-PWD-NBE) and by using the modified ion exchange method (MIE-PWD) of Poeppelemeier et al. [14] after reduction at 500°C.

over either of the two IE preparations, as indicated by the greater fraction of low wavenumber Pt-carbonyl bands.

We then investigated the role of excess water during the IWI preparation procedure. No major shifts in peak positions were observed for the catalysts prepared with excess water.

Attention was also focused on preparation procedure that may lead to a large-scale implementation of the VPI method. We investigated the use of the mechanical pump (VPI-PWD-MP) and the helium flow (VPI-PWD-HEF) preparations for the powder catalysts. Fig. 3 shows the results after reduction at 500°C for the two catalysts in comparison with the high vacuum procedure. All VPI catalysts displayed a large fraction of bands between 2010–1930 cm<sup>-1</sup> associated with stabilized Pt-carbonyls. In addition, clear bands

at 2033, 2053, and 2064 cm<sup>-1</sup> were also observed. The shoulder at 2064 cm<sup>-1</sup> was more pronounced for the VPI-PWD-MP preparation, with a contribution from a band present at 2069 cm<sup>-1</sup>. Finally, we utilized FTIR of adsorbed CO to characterize three different preparation methods conducting the incorporation of the Pt directly on the pre-formed pellets. The results were very different in comparison with the powder catalysts. Unfortunately, and as expected, all the pellet catalysts showed a substantial contribution of high wavenumber bands. All of them displayed a shoulder or peak at 2080 cm<sup>-1</sup> or higher. As an example, we can compare catalysts prepared by VPI and the standard IE method in the pellet form SIE-PEL-NBE. In Fig. 4, the VPI-PEL-HEF displays a small fraction of bands associated with the formation of Pt-carbonyls, while the standard IE pellet catalyst does not show any. Both

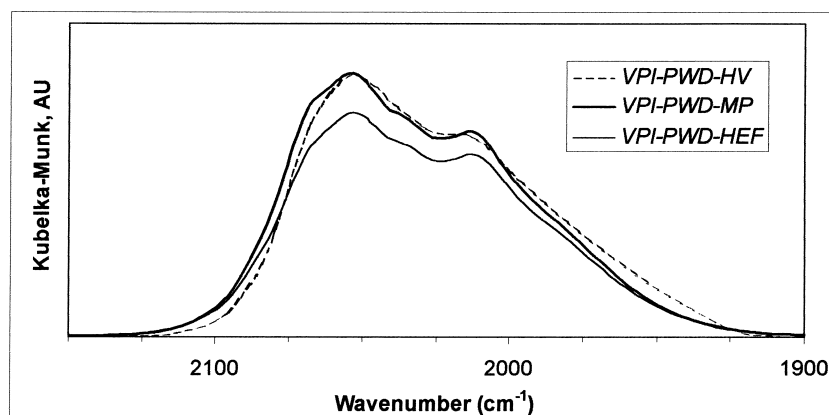


Fig. 3. DRIFTS spectra of CO adsorbed on the catalysts prepared by vapor phase impregnation under high vacuum,  $10^{-5}$  Torr (VPI-PWD-HV), moderate vacuum,  $10^{-3}$  Torr (VPI-PWD-MP), and under flow of He (VPI-PWD-HEF) after reduction at  $500^{\circ}\text{C}$ .

presented peaks at  $2065\text{ cm}^{-1}$  and between  $2080$  and  $2084\text{ cm}^{-1}$ , reflecting a large number of particles outside the channels of the zeolite. Note that the modified ion exchange method [14] was not carried out on extrudates in this work, and would likely result in a much improved IE pellet catalyst, in light of the results in Fig. 2b for powder catalysts.

### 3.2. Catalytic testing of *n*-hexane aromatization in a flow reactor

#### 3.2.1. Powder catalysts

The three catalyst preparation methods displayed significant differences in their deactivation patterns

for the aromatization of *n*-hexane reaction at  $450^{\circ}\text{C}$ . Fig. 5 shows the benzene yield for the SIE-PWD-NBE, IWI-PWD, and VPI-PWD-HV catalysts at 10 min, 1.5 h, and 9 h on stream. The SIE-PWD-NBE showed a low aromatization activity and a low stability. Similarly, as in previous testing [12,21], the IWI showed a significant drop in initial activity, not as pronounced as the IE, but significantly worse than the VPI catalyst. As expected, the differences correlated well with important differences in the production of methane and hexenes. That is, the VPI resulted in higher aromatization selectivities, lower production of hexene intermediates, lower hydrogenolysis activity, and a lower deactivation rate.

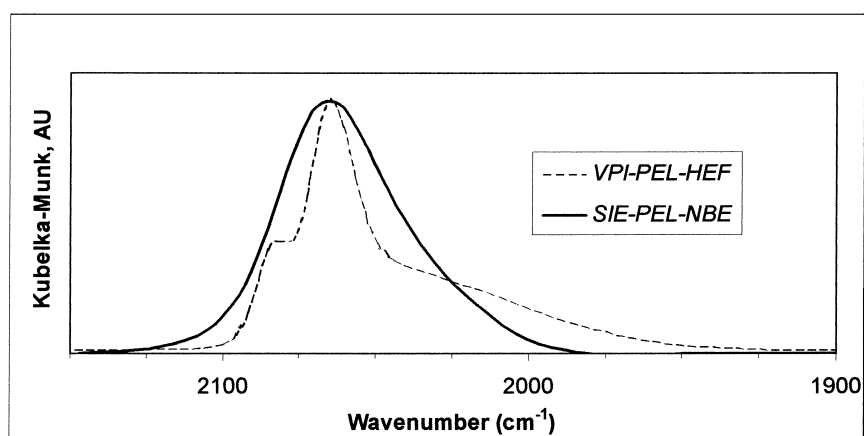


Fig. 4. DRIFTS spectra of CO adsorbed on pelletized vapor phase impregnation helium flow VPI-PEL-HEF and standard ion exchange without back-exchange SIE-PEL-NBE catalysts after reduction at  $500^{\circ}\text{C}$ .

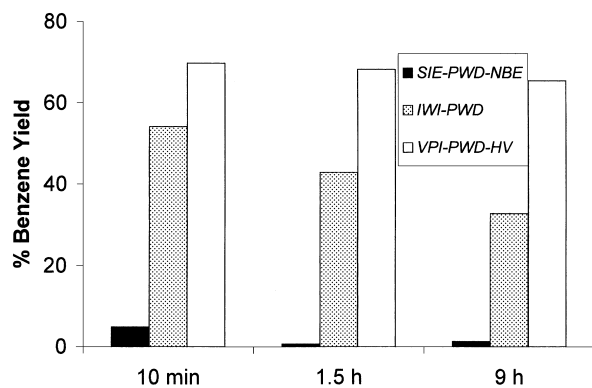


Fig. 5. Benzene yield vs. time onstream obtained under flow conditions ( $T$ : 450°C, WHSV: 10 h<sup>-1</sup>,  $P$ : 1 atm) on powder catalysts prepared by the standard ion exchange method without back-exchange (SIE-PWD-NBE), incipient wetness impregnation (IWI-PWD), and vapor phase impregnation high vacuum (VPI-PWD-HV).

A comparison of the VPI-PWD-HV and IWI-PWD catalysts was also conducted at 500°C, a temperature which is commonly reported in the literature for catalytic testing of Pt/KL. Results of catalytic testing, shown in Fig. 6, indicate a much higher hydrogenolysis at 500°C in comparison with the results obtained at 450°C. To determine whether the loss in aromatization selectivity at 500°C was due to an irreversible Pt particle growth or simply to kinetic reasons, we conducted the following experiment. First, we tested the VPI catalyst at 450°C, increased the temperature

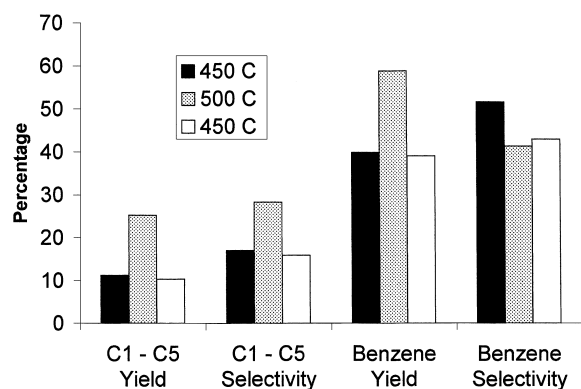


Fig. 6. Yield and selectivities of hydrogenolysis (C1–C5) and benzene for a Pt (1%)/IWI catalyst tested for *n*-hexane aromatization at 450°C, followed by ramping and testing at 500°C, and then reducing the temperature back to 450°C and testing one final time.

and tested at 500°C, and then reduced the temperature to 450°C to take the final measurement. The result was that increasing the temperature led to an increase in hydrogenolysis. After reducing the temperature back to 450°C, the hydrogenolysis pathway was as low as before. Results are reported in Fig. 6. For a well-prepared catalyst, 450°C appears as an appropriate choice for aromatization, yielding satisfactory activity and selectivity. Higher temperatures, may yield higher conversion, but they are detrimental for selectivity and particularly stability. However, a word of caution is important since this conclusion was drawn from data obtained at near-atmospheric pressure and it may not hold valid under the high pressures employed in the industrial process.

In order to test the effect of excess water on the preparation of IWI catalysts, comparisons were made for the IWI-PWD, IWI-PWD-EXP, IWI-PWD-XS, and IWI-PWD-NCL catalysts. Reaction results for the four catalysts are displayed in Fig. 7. The IWI-PWD-EXP catalyst, which contained water in the pores before impregnation, but was then impregnated just to incipient wetness, did not show any marked difference with the IWI-PWD catalyst. However, the IWI-PWD-XS and IWI-PWD-NCL catalysts, which were filled beyond incipient wetness, clearly displayed

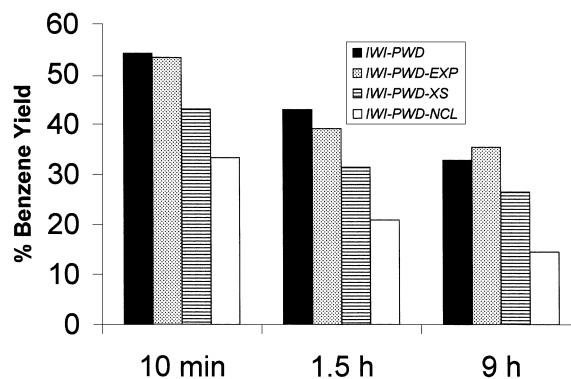


Fig. 7. Benzene yield vs. time onstream under *n*-hexane aromatization flow conditions ( $T$ : 450°C, WHSV: 10 h<sup>-1</sup>,  $P$ : 1 atm) for IWI powder catalysts prepared by calcining and keeping the L-zeolite very dehydrated before salt solution addition (IWI-PWD), exposing calcined L-zeolite to ambient conditions before salt solution addition (IWI-PWD-EXP), exposing calcined L-zeolite to ambient conditions and overfilling during salt solution addition (IWI-PWD-XS), and without calcination of the L-zeolite prior to salt solution addition (IWI-PWD-NCL).

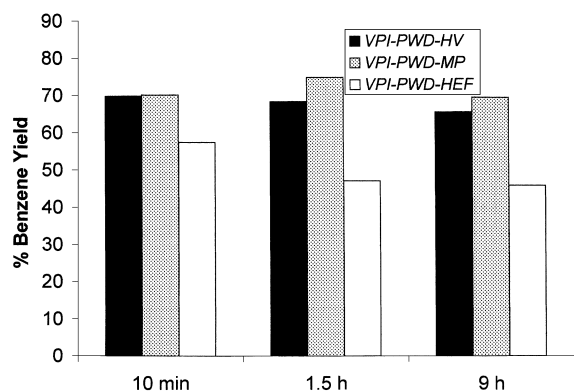


Fig. 8. Benzene yield vs. time onstream under *n*-hexane aromatization flow conditions ( $T$ : 450°C, WHSV: 10 h<sup>-1</sup>,  $P$ : 1 atm) for VPI powder catalysts prepared by using high vacuum (VPI-PWD-HV), a mechanical pump vacuum (VPI-PWD-MP), and under helium flow (VPI-PWD-HEF).

lower activity and a more significant deactivation than catalysts filled to incipient wetness. These results correlated well with hydrogen chemisorption data, which showed lower H/Pt values for the catalysts prepared with excess water. Therefore, excess water during IWI preparation results in a distribution of Pt with greater sensitivity to particle growth during the reduction step.

Testing was further conducted on the different VPI preparation methods. Comparisons are shown in Fig. 8 for the VPI-PWD-MP, VPI-PWD-HEF, and VPI-PWD-HV catalysts. In line with hydrogen chemisorption and FTIR of adsorbed CO results, no notable differences were detected between the VPI-PWD-HV and VPI-PWD-MP catalysts. The VPI-PWD-HEF catalyst exhibited a somewhat lower yield but most of this difference is due to a lower metal loading. In this preparation, the Pt precursor was physically mixed to obtain a loading of 1% Pt, but the final loading was determined to be 0.89%, evidencing some loss of metal during the sublimation under flow.

### 3.2.2. Pellet catalysts

Results for the pellet catalysts are reported in Fig. 9. Although the impregnation catalysts, and especially the vapor phase impregnation catalysts, showed good catalytic performance for the powder preparation, these attributes were not reproduced when the incorporation of the metal was done on the pellet. It is

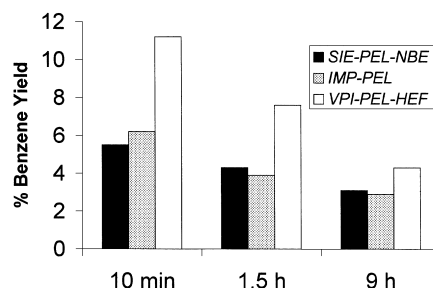


Fig. 9. Benzene yield vs. time onstream under *n*-hexane aromatization flow conditions ( $T$ : 450°C, WHSV: 10 h<sup>-1</sup>,  $P$ : 1 atm) for pelletized catalysts prepared by the standard ion exchange method (SIE-PEL-NBE), dip impregnation (IMP-PEL), and vapor phase impregnation using helium flow (VPI-PEL-HEF).

possible that even if the initial activity may have been relatively high, the deactivation of these catalysts is so rapid that by the time the first data point was obtained they had virtually deactivated. A similar behavior was reported in our previous work for nonmicroporous Pt/SiO<sub>2</sub> and Pt/Mg(Al)O catalysts, which exhibited comparable aromatization activities in the pulse-mode operation, but quickly deactivated under flow [21].

## 4. Discussion

The purpose of this work was to study how different preparation procedures affected the resulting distribution of Pt cluster size and location, and to correlate these changes with the resulting catalytic performance and stability of Pt/KL powder and pellet catalysts for the aromatization of *n*-hexane. We can first analyze the results of the characterization methods and interpret the wide range in activity and stability displayed by the catalysts when we systematically varied the method of incorporation of Pt. We will then discuss the implications of these results in the production of effective industrial Pt/KL catalysts.

Hydrogen chemisorption results demonstrate that with all preparation techniques employed, the Pt clusters were very highly dispersed. However, important changes in the overall stability of the various samples were observed under the flow reaction. Therefore, dispersion measurements alone are not good indicators of a well-prepared catalyst. Therefore, we attempted to determine the size and location distributions of the

catalysts to find out if this distribution can be correlated with catalytic performance and stability. As mentioned, FTIR of adsorbed CO is a tool that probes the location (i.e. inside the L-zeolite or external) and distribution of the Pt clusters loaded to KL [16]. As discussed previously, a broad distribution of bands (2080–1930  $\text{cm}^{-1}$ ) for linearly bonded CO has been observed for Pt/KL catalysts. As discussed in the previous section, this distribution can be divided into three important regions: (1) bands below 2050  $\text{cm}^{-1}$  are assigned to Pt–CO species arising from the disruption of small Pt clusters inside the L-zeolite channels; (2) bands between 2050 and 2075  $\text{cm}^{-1}$  are associated with larger Pt clusters in the near-surface region of the L-zeolite; and (3) bands at around 2080  $\text{cm}^{-1}$  are in general assigned to larger Pt particles on the external surface of the L-zeolite.

The assignments are not only useful for probing the state of Pt clusters at a specific temperature (e.g. a temperature required for a specific reaction), but they also give dynamic information about the resistance of Pt clusters to agglomeration when the reduction temperature is increased. This resistance is related not only to the cluster size, but also to the location (internal or external as well as distance from the pore mouth) of the cluster and its proximity relative to neighboring clusters. This information is particularly useful for screening different preparations of Pt/KL catalysts.

From Fig. 1a and b and by examining Table 3, it is evident that after reduction at 400°C, a large fraction of Pt clusters in the standard IE catalyst (SIE-PWD-NBE) are either outside the L-zeolite channels or close to the pore mouth. Only a small fraction of Pt-carbonyls was observed at 2033 and 2010  $\text{cm}^{-1}$ , while lower wavenumber bands are absent almost entirely. However, after reduction at 500°C, the spectrum is drastically shifted to even higher wavenumbers, and the peak at 2080  $\text{cm}^{-1}$  dominates the spectrum, accounting for 64% of the total intensity. These results suggest that with the standard ion exchange procedure, the Pt particles end up close to the mouth of the pores. The sensitivity to high temperature treatment suggests that the Pt particles were in close proximity to one another, resulting in agglomeration. The near-surface species also migrated after the high temperature treatment to the external surface of the L-zeolite. Fig. 2a shows that the back-exchange procedure, which is normally effective in removing unwanted acidity, offers no real

improvement in Pt cluster morphology. Similarly, the IE pellet catalyst prepared by the standard ion exchange method (Fig. 4) displayed poor characteristics. Fig. 2b shows, however, that the modified IE catalyst displays a greater fraction of low wavenumber bands after reduction at 500°C than the standard IE catalyst, and shows virtually no bands associated with external Pt, in contrast with the standard IE catalyst. It is clear that the aging step during preparation aids in dispersing the salt throughout the channels. It is likely that these characteristics are carried over to extrudates.

The IWI procedure offers a marked improvement over the standard IE method. Fig. 1a and b illustrate that except for a small fraction as indicated by a slight shoulder at 2075–2080  $\text{cm}^{-1}$ , virtually all of the Pt is located inside the channels of the L-zeolite. After reduction at 400°C, little differences are observed in the spectra in comparison with the VPI catalyst. However, increasing the reduction temperature to 500°C demonstrates that the IWI catalyst is more susceptible to agglomeration than the VPI. This is indicated by the growth in bands between 2050 and 2075  $\text{cm}^{-1}$  and the loss of the bands associated with Pt-carbonyls, as quantified in Table 3. In our previous study [12], we showed by EXAFS, MCP-RO, and TEM that a fraction of particles large enough to block the channels exists for IWI catalysts after reduction at 500°C. While the IWI procedure incorporates small clusters into the L-zeolite, it appears that after preparation, a fraction of the clusters are in close proximity to one another. After high temperature treatment, this fraction of small particles, located near the mouth of the pore, agglomerates to fill and partially block the channels.

Further improvement in catalyst preparation was achieved with the VPI procedure. Fig. 1a shows that after reduction at 400°C, not only most of the Pt in this catalyst is located inside the channels of the L-zeolite, but this sample also shows the highest intensity of bands in the range of Pt-carbonyls. Besides, as shown in Fig. 1b and Table 3, after reduction at 500°C, the bands do not display a marked shift to higher wavenumbers as the other catalysts do. Again, these results are consistent with our previous VPI results from EXAFS, which displayed lower Pt–Pt coordination and higher Pt coordination to zeolite lattice oxygen atoms in comparison with IWI catalysts [12]. MCP-RO showed that the Pt clusters were small enough such that collimation effects were not

observed, in contrast with the catalysts prepared by IWI.

Therefore, we conclude that the VPI preparation procedure results in small Pt clusters that are more evenly distributed throughout the L-zeolite channels than those produced from the IWI and IE methods. The results of FTIR after reduction treatment at 500°C suggest that the VPI procedure does not selectively deposit a greater fraction of Pt clusters at the near-surface region, in contrast with the IWI and standard IE catalysts. The Pt clusters in this region are located further apart for the VPI catalyst, resulting in a catalyst that is more resistant to agglomeration at high temperature. Note that the modified IE powder (MIE-PWD) catalyst shows a considerable improvement in Pt cluster morphology over the standard method. However, the fraction of Pt carbonyl bands in the low wavenumber region were considerably lower than the VPI powder catalysts, indicating the VPI is a marked improvement over even the modified IE method for preparation on the powder.

The use of a moderate vacuum (e.g. mechanical pump) or a low helium flow to prepare the VPI powder catalyst results in a catalyst with a similar distribution to the catalyst prepared using high vacuum (Fig. 3). However, as shown in Fig. 4, preparation on the pellet results in a considerable fraction of Pt external to the L-zeolite and likely on the binder. The fraction of bands associated with Pt-carbonyls was much lower than on the VPI powder catalysts. The implication of these results is very important. Using the VPI preparation method directly on L-zeolite pellets does not lead to a catalyst with improved catalytic properties. However, if a method existed to prepare pellets extruded directly from the VPI powder catalyst without affecting the Pt clusters, the result would likely be a major development.

#### 4.1. Catalytic performance and stability

Fig. 5 shows that under *n*-hexane flow reaction at 450°C and  $WHSV=10\text{ h}^{-1}$ , the standard IE catalyst rapidly deactivates. In fact, by the time the first point was taken at 10 min, the catalyst had already virtually deactivated. In conjunction with FTIR results, which demonstrate a considerable fraction of external Pt and large clusters at the pore mouth, and considering the dark appearance of the catalyst after reaction, it is clear

that the catalyst deactivates by coke formation. This result is in agreement with the interpretation by Iglesia and Baumgartner [11]; they proposed that external Pt is susceptible to bimolecular reaction pathways which lead to the formation of coke.

In contrast to the standard IE catalyst, Fig. 5 shows that the deactivation of the IWI catalyst is a slower process. The catalyst approaches steady state after approximately 9 h on stream. Results from FTIR show that Pt is mostly located inside the channels of the L-zeolite. Therefore, the mechanism of deactivation is not simply coking of external Pt. The high temperature reduction treatment in the FTIR study demonstrates that the Pt clusters from the IWI procedure have a fraction which is prone to agglomeration in the near-surface region of the channels. This agglomeration accounts for the slow deactivation of the catalyst to a benzene yield which is approximately half that of the VPI catalyst after 9 h on stream.

Further evidence for this mode of deactivation, reported elsewhere in the literature [22], is provided by examining the IWI catalysts prepared with excess water. In the FTIR results (not shown), the band positions were the same as the standard IWI catalyst. However, results of hydrogen chemisorption (Table 2) demonstrate that these catalysts are more sensitive to Pt particle growth after high temperature reduction, and especially in the case of the catalyst prepared without dehydrating the L-zeolite support. This indicates a fraction of the Pt deposited selectively near the pore mouth, resulting in smaller distances between Pt clusters after the calcination and reduction steps.

FTIR results for the dip impregnation pellet catalyst were not shown for clarity. However, the presence of a large fraction of bands at  $2080\text{ cm}^{-1}$  and only a small contribution from the Pt-carbonyl range indicated a significant fraction of external Pt. Therefore, the Pt likely deposited in large part on the binder. Reaction testing (Fig. 9) is in agreement with those findings. The catalyst deactivated rapidly by the formation of coke.

As demonstrated in Figs. 5 and 8, the VPI catalysts displayed the highest activity and selectivity and the lowest deactivation rates. FTIR results showed that in addition to the Pt being located inside the L-channels, the Pt clusters were also more resistant to high temperature reduction. Therefore, under reaction, the catalysts showed little or no evidence for deactivation from

agglomeration of Pt. The VPI catalysts prepared by moderate vacuum (VPI-PWD-MP) performed as well as the high vacuum catalyst (VPI-PWD-HV). However, the helium flow VPI catalyst (VPI-PWD-HEF) showed slightly lower activity. This difference can be explained by the fact that a fraction of the Pt precursor was lost during the sublimation procedure (Table 1). The helium flow procedure resulted in a lower loading of Pt than the vacuum preparation techniques. It is important to note that the L-zeolite must be kept moisture free during the VPI preparation. We have observed previously that introducing traces of water into the L-zeolite by exposure to ambient conditions prior to sublimation of the Pt acetylacetonate results in a catalyst that deactivates under *n*-hexane aromatization.

The VPI pellet catalyst, which displayed a considerable fraction of near-surface and external Pt from FTIR, deactivated almost completely during 9 h under flow reaction. This demonstrates further that the VPI procedure is ineffective when directly conducted on extrudates. However, preparation of the pellet directly from extruding the VPI powder catalyst may lead to a good catalyst for commercial scale-up.

## 5. Conclusions

The method of preparation and the choice of either powder or pellet for the support strongly influence the resulting Pt cluster size and location distribution. All powder catalysts — IE, IWI, and VPI — were found to exhibit high H/Pt ratios, all of which were greater than unity. However, FTIR of adsorbed CO showed that, more important than dispersion, it is the distribution of Pt cluster size and location that influences the activity and stability of the catalyst for the *n*-hexane aromatization reaction.

For catalysts reduced at 400°C, FTIR showed that the IE catalyst prepared by the standard method had a large fraction of Pt external to the L-zeolite. In contrast, the IWI and VPI catalysts displayed virtually all of the Pt inside the L-zeolite channels. After reduction at 500°C, the catalysts displayed differences in sensitivity to the treatment. Our standard IE catalysts showed growth in bands at high wavenumbers indicative of Pt migration out of the L-zeolite channels. These catalysts rapidly deactivated by coke formation. An ion exchange catalyst with improved

Pt cluster morphology was also prepared using a modified ion exchange procedure found in the patent literature. In that case, an aging step allows the salt to distribute inside the channels of the L-zeolite, as revealed by DRIFTS of adsorbed CO. IWI catalysts also displayed growth in bands assigned to Pt clusters inside the channels, but near the surface. The IWI catalysts were found to slowly lose activity, reaching a steady state activity approximately half that of the initial activity. VPI catalysts maintained low wavenumber bands after high temperature reduction, indicating that the small Pt clusters were more evenly distributed, and not localized near the pore mouth. These catalysts showed the highest activity and selectivity, with long-term stability. The IWI and IE catalysts were also less reproducible than the VPI preparation.

Reaction testing and characterization demonstrated that the VPI catalyst could be scaled-up using either a moderate vacuum or a helium flow preparation method. These catalysts displayed very little differences from the high vacuum preparation method when probed with FTIR of adsorbed CO. No differences in activity or stability were observed between the catalyst prepared by moderate or high vacuum. The catalyst prepared by the helium flow VPI method showed no differences in band positions, but 10% of the Pt was lost during the preparation procedure. Preparation directly on the pellets resulted in a large fraction of Pt external to the pores and likely on the binder for the methods studied in this work — standard IE, IWI, and VPI. However, in light of the results of DRIFTS of adsorbed CO for the powder catalyst, it is likely that the modified IE method could result in a pelletized catalyst with better characteristics than the one prepared by the standard IE method. Finally, preparation of the pellet directly from extruding the VPI powder catalyst may lead to a good catalyst for commercial use.

## Acknowledgements

This work was supported by the Oklahoma Center for the Advancement of Science and Technology (OCAST). We acknowledge the National Science Foundation for a GRT traineeship for one of us (GJ) and Phillips Petroleum for a scholarship.

## References

- [1] C.V. Besoukhanova, J. Guidot, D. Barthomeuf, M. Breysse, J.R. Bernard, *J. Chem. Soc., Faraday Trans. 1* 77 (1981) 1595.
- [2] K.J. Ostgard, L. Kustov, K.R. Poeppelmeier, W.M.H. Sachtler, *J. Catal.* 133 (1992) 342.
- [3] I. Manninger, Z. Paal, B. Tesche, U. Klengler, J. Halasz, I. Kiricsi, *J. Mol. Catal.* 64 (1991) 361.
- [4] A.E. Schweizer, US Patent 4,992,401 (1991).
- [5] S.B. Hong, E. Mielczarski, M.E. Davis, *J. Catal.* 134 (1992) 349.
- [6] C. Dossi, R. Psaro, A. Bartsch, A. Fusi, L. Sordelli, R. Ugo, M. Bellatreccia, R. Zanoni, G. Vlaic, *J. Catal.* 145 (1994) 377.
- [7] G. Larsen, G.L. Haller, *Catal. Today* 15 (1992) 431.
- [8] L.X. Dai, H. Sakashita, T. Tatsumi, *J. Catal.* 149 (1) (1994) 246.
- [9] G. Larsen, Ph.D. Thesis, Yale University, 1992.
- [10] W.E. Alvarez, D.E. Resasco, *J. Catal.* 164 (1996) 467.
- [11] E. Iglesia, J.E. Baumgartner, in: *Proceedings of the 10th ICC*, 19–24 July, 1992, Budapest, Hungary.
- [12] G. Jacobs, F. Ghadiali, A.P. Pisanu, A. Borgna, W.E. Alvarez, D.E. Resasco, *Appl. Catal. A* 188 (1999) 79.
- [13] G. Jacobs, F. Ghadiali, A. Pisanu, C. Padro, A. Borgna, W.E. Alvarez, D.E. Resasco, *J. Catal.*, in press.
- [14] K.L. Poeppelmeier, T.D. Trowbridge, J.L. Kao, US Patent 4,568,656 (1986).
- [15] B.J. McHugh, G. Larsen, G.L. Haller, *J. Phys. Chem.* 94 (1990) 8621.
- [16] A.Y. Stakheev, E.S. Shpiro, N.I. Jaeger, G. Schulz-Ekloff, *Catal. Lett.* 34 (1995) 293.
- [17] B.L. Mojet, Ph.D. Thesis, University of Utrecht, June 16, 1997.
- [18] B.L. Mojet, J.T. Miller, D.C. Koningsberger, *J. Phys. Chem. B* 103 (1999) 2724.
- [19] S.C. Fung, US Patent 5,106,798 (1992).
- [20] B.L. Mojet, D.C. Koningsberger, *Catal. Lett.* 39 (1996) 191.
- [21] G. Jacobs, C.L. Padro, D.E. Resasco, *J. Catal.* 179 (1998) 43.
- [22] M.M.J. Treacy, *Microporous Mesoporous Mater.* 28 (1999) 271.